Batch Extraction of Amines Using Emulsion Liquid Membranes: Importance of Reaction Reversibility

Experimental results for the batch extraction of amines using emulsion liquid membranes with an internal aqueous HCl solution are presented. Four amines and mixtures of one binary pair were studied. Reversibility of the acid-amine reaction within the internal droplets affected extraction rates. The reversible reaction model presented earlier satisfactorily predicts these experimental results.

R. S. Baird, A. L. Bunge
Colorado School of Mines
Golden, CO 80401

R. D. Noble
National Bureau of Standards
Center for Chemical Engineering
Boulder, CO 80303

Introduction

Emulsion liquid membranes (ELM) are double emulsions formed by emulsifying two immiscible phases and then dispersing this emulsion in another continuous phase under agitation. While ELM technology has existed for nearly 100 years, Li (1968) was the first to apply it as a separation technique. Since then, liquid membranes have been applied to a variety of separations, including recovery and purification of metal ions, removal of organic contaminants from wastewater, and various biochemical and biomedical applications.

This paper considers ELM extraction by solute diffusion through the oil membrane followed by reaction with reagent present in the internal droplets. Examples of this mechanism are the extraction of organic acids such as phenol, cresols, or acetic acid into basic internal droplets, or the extraction of basic solutes, amines, or ammonia into acidified internal droplets.

Recently, several mathematical models have been presented that more realistically represent the composite nature of the emulsion globule. The advancing front model developed by Ho et al. (1982) assumes that the reaction between solute and internal reagent is irreversible. Stroeve and coworkers (Stroeve and Varanasi, 1984; Fales and Stroeve, 1984), and Kim et al. (1983) extend Ho's approach to include mass transfer resistances external and internal to the globule surface, respectively. The models described by Teramoto et al. (1981, 1983) and Bunge and Noble (1984) remove the restriction of irreversibility. To date, these theories have been used only to predict extraction from solutions containing a single solute.

Correspondence concerning this paper should be addressed to A. L. Bunge.

Several parameters must be known to compare experimental and model predictions: the area-averaged (Sauter mean) globule diameter, the solute phase equilibrium between the membrane and the bulk or internal phases, and the effective coefficient for solute diffusion through the composite globule. The reversible reaction approaches of Teramoto and Bunge also require reaction equilibrium constants. Of the body of appropriate experimental data, many do not report or provide sufficient information to estimate these parameters.

Several experimental studies that did measure and report the necessary parameters have other limitations. For example, in one procedure the bulk phase already contains the transferring solute when the emulsion is added; in another procedure, solute addition to the previously dispersed emulsion significantly changes the bulk phase volume. In both cases globule diameters will vary during the first few minutes of extraction. This variation complicates any theoretical interpretation, particularly when most of the extraction occurs in the first few minutes.

Other complications arise when the extraction proceeds too quickly; the experimental results depend critically on the sampling procedure and how rapidly the emulsion and bulk phases are separated. Furthermore, when extraction rates are large, external mass transfer resistance can contribute significantly and must be included in the comparative model. For purposes of evaluating theoretical analyses, the experimental system and procedure should insure stable globules of constant diameter and sufficiently slow extraction rates to permit reliable sampling.

The major objective of this study was to examine the importance of reaction reversibility on ELM performance. Experimental data for extraction from solutions of single amines and

mixtures of amines were measured. The experimental system and procedure were designed to provide a reasonable test of the reversible reaction model proposed by Bunge and Noble (1984). Using a high-viscosity membrane phase insured that extraction rates were reasonably slow to facilitate sampling. Estimates of the Biot modulus (always greater than 1,000) confirm that diffusional resistances control (Skelland and Lee, 1981; Fales and Stroeve, 1984). Small samples of high-concentration solute were added to the predispersed emulsion of unvarying average radius.

The extension of the Bunge-Noble model to solutions of mixed solutes is also described. Besides comparison with experimental mixtures, batch extraction curves are generated for binary systems of hypothetical solutes. These results show that solubility of solute in the membrane and reaction reversibility are both important factors. For some combinations of these two effects, the concentration vs. time curve can display minimum values.

Batch Extraction Theory

Recent mathematical descriptions of ELM extractions that involve solute A reaction with an internal phase reagent B to produce a product P:

$$A + B \overset{K}{\rightleftharpoons} P \tag{1}$$

have been formulated in two ways. One approach described by Ho et al. (1982) assumes that the solute removed from the bulk phase diffuses through the membrane globule to a reaction front, where it is removed instantaneously and irreversibly by reaction with the internal reagent. That is, the equilibrium constant, K, for reaction 1 is assumed to be infinitely large. In turn, the reaction front progresses toward the center as internal reagent is consumed. We refer to this approach as the advancing front model.

An alternate procedure, taken by Bunge and Noble (1984) as well as by Teramoto et al. (1981), incorporates reaction equilibrium into a description of the rate-controlling membrane transport processes. These reversible reaction models predict interdependent solute, reagent, and product concentrations.

Several assumptions are common to both the advancing front and the reversible reaction approaches:

1. The membrane and bulk phases as well as membrane and internal phases are totally immiscible.
2. Local phase equilibrium holds between membrane and droplet phases.
3. No internal circulation occurs within the globule.
4. Globule size variations can be lumped into a single effective mean diameter.
5. The system is well-agitated, eliminating external bulk phase mass transfer resistance.
6. Internal droplets can be treated as uniformly dispersed, immobile solute sinks of finite capacity.
7. Diffusion within the membrane is slow relative to the rate of phase distribution and chemical reaction. Consequently, the internal phase droplets are always in phase and reaction equilibrium with the local membrane concentration of solute.
8. Membrane breakage is neglected.

Teramoto's reversible reaction model includes external mass transfer resistances, as does the extension by Stroeve and coworkers (Stroeve and Varanasi, 1984; Fales and Stroeve, 1984) of Ho's advancing front theory. Besides this external mass transfer resistance, Kim and coworkers (1983) and Teramoto et al. (1981, 1983) also incorporated an additional membrane film resistance that is meant to simulate the observation that internal water droplets cannot reach the surface of the emulsion globule. The model of Kim et al. requires this additional resistance because their technique of volume-averaging the internal and membrane diffusion coefficients underestimates the diffusive resistance for their conditions. For their system (kerosene, amines, and HCl), Teramoto et al. (1981) discovered that the peripheral oil layer contribution is negligible.

Advancing front model

The advancing front model of Ho et al. depends on two dimensionless parameters, ϵ and E. Physically, E is three times the original mole ratio of internal reagent to bulk solute. For long times, if $E/3$ is greater than one then there is sufficient reagent to completely remove the solute and no equilibrium is established. If $E/3$ is less than one, there is insufficient reagent and solute phase equilibrium is assumed. The second dimensionless group, ϵ, measures the globule capacity for unreacted solute relative to the reaction capacity provided by the reagent. The value of ϵ is generally much less than 1.0. A notable feature of the advancing front theory is its algebraic solution, permitting easy calculation. One limitation of this approach is the assumption of reaction irreversibility, which when combined with instantaneous kinetics requires that the reagent concentration be identically zero in the reacted region. This situation is asymptotically achieved only for large K and large solute concentrations. The reversible reaction models remove this restriction.

Reversible reaction models

Reaction reversibility precludes the advancing front since there are no separate reacted and unreacted regions. Solute diffusing into the emulsion globule either reacts with the internal reagent or distributes itself between the two phases. The membrane-insoluble product formed inside the encapsulated droplets is capable of the reverse reaction, producing unreacted solute that can diffuse back into the membrane. Thus, it is conceivable that solute could diffuse to the center of the globule without contacting the internal reagent or through a series of forward and reverse reaction steps.

The earliest model allowing reaction reversibility was developed by Teramoto and coworkers (1981, 1983). Because of low stirring rates and moderately high diffusion coefficients in their studies, external mass-transfer resistances did contribute to extraction rates and were determined experimentally, as was their effective diffusion coefficient. These experimentally determined effective diffusion coefficients were compared with those estimated using the Russell equation, which is similar to the Jefferson-Witzell-Sibbett (JWS) equation used here (see Appendix A) and elsewhere (Ho et al., 1982; Bunge and Noble, 1984). The chief difference between the Russell and JWS developments is the geometry of the dispersed phase; Russell assumes a cube while Jefferson and coworkers use a cylinder.

These estimated diffusion coefficients do not compare well with their experimentally determined values because the estimation technique does not include the apparent enhancement of the internal phase diffusivity by diffusion of the reacted species

(Teramoto et al., 1981, 1983). As noted by Teramoto and coworkers, the differences between experimental and estimated diffusion coefficients should indicate the extent to which solute reaction enhances the effective diffusivity. Because the amount of reaction depends on the local concentrations of solute and reagent, we expect the effective diffusivity to vary with feed and reagent concentrations. Strictly then, Teramoto's approach requires an experimentally determined effective diffusion coefficient measured near the concentrations of interest.

Mathematical description of reversible reaction model

A reversible reaction model with no adjustable parameters was developed by Bunge and Noble (1984). Based on an approach similar to that of Teramoto, the dimensionless solute concentration in the membrane phase of the globule, ϕ_m, and in the continuous, bulk phase, ϕ_b, are given as:

Globule:

$$\frac{\partial \phi_m}{\partial \tau} = \frac{1}{\eta^2}\frac{\partial}{\partial \eta}\left(\eta^2 \frac{\partial \phi_m}{\partial \eta}\right)\left\{\frac{1}{1 + (\sigma_2/\sigma_1)[1 + \sigma_3/(1 + \sigma_4\phi_m)^2]}\right\} \tag{2}$$

$$\tau = 0 \qquad \phi_m = 0 \qquad (1 > \eta \geq 0) \tag{3}$$

$$\eta = 1 \qquad \phi_m = \phi_b \qquad (\tau \geq 0) \tag{4}$$

$$\eta = 0 \qquad \partial \phi_m / \partial \eta = 0 \qquad (\text{all } \tau) \tag{5}$$

Bulk phase:

$$\frac{d\phi_b}{d\tau} = -3\sigma_1 \left.\frac{\partial \phi_m}{\partial \eta}\right|_{\eta = 1} \tag{6}$$

$$\tau = 0 \qquad \phi_b = 1 \tag{7}$$

where

$$\eta = \frac{r}{R}; \qquad \tau = (\bar{D}_{\text{eff}})\frac{t}{R^2} \tag{8}$$

$$\phi_b = \frac{C_{Ab}}{C^\circ_{AB}}; \qquad \phi_m = \frac{C_{Am}}{C^\circ_{Ab} K_{mb}} \tag{9}$$

$$\sigma_1 = f_m[(1 - f_b)/f_b]K_{mb} \tag{10}$$

$$\sigma_2 = (1 - f_m)[(1 - f_b)/f_b]K_{mb}/K_{mi} \tag{11}$$

$$\sigma_3 = KC^\circ_{Bi} \tag{12}$$

$$\sigma_4 = K K_{mb} C^\circ_{Ab}/K_{mi} \tag{13}$$

Here R is the globule radius, f_m is the membrane fraction of the globule volume, f_b is the bulk fraction of the total volume, and K_{mb} and K_{mi} are solute partition coefficients between the membrane/bulk and membrane/internal phases, respectively. The mean effective diffusivity based on the membrane driving force, $\bar{D}_{\text{eff}}$, must include the effects of diffusion through a composite medium plus contribution from reaction; see Appendix A. The physical meaning of the dimensionless groups defined in Eqs. 10–13 is significant. The membrane capacity for solute relative to the bulk phase capacity is represented as σ_1, while σ_2 is a measure of the internal phase capacity for unreacted solute relative to the bulk phase capacity. The original internal reagent and bulk solute concentrations are specified by dimensionless groups σ_3 and σ_4, respectively.

Model extension to multicomponent mixtures

The reversible reaction model was extended to include the effects of multicomponent mixtures on the extraction rates of the individual components. In dimensionless form, the equations describing concentrations of a solute j in the membrane portion of the globule and in the continuous bulk phase are:

Membrane phase:

$$\frac{\partial \phi_{mj}}{\partial \tau} = \frac{1}{\psi_j}\left[\beta_j \frac{1}{\eta^2}\frac{\partial}{\partial \eta}\left(\eta^2 \frac{\partial \phi_{mj}}{\partial \eta}\right) + \frac{\sigma_{3_j}\left(\frac{\sigma_2}{\sigma_1}\right)_j \sum_{\substack{k=1 \\ k \neq j}}^{n}\left(\sigma_{4_k}\phi_{mj}\frac{\partial \phi_{mk}}{\partial \tau}\right)}{\left(1 + \sum_{k=1}^{n}\sigma_{4_k}\phi_{mk}\right)^2}\right] \tag{14}$$

where

$$\psi_j = 1 + \left(\frac{\sigma_2}{\sigma_1}\right)_j\left[1 + \frac{\sigma_{3_j}\left(1 + \sum_{\substack{k=1 \\ k \neq j}}^{n}\sigma_{4_k}\phi_{mk}\right)}{\left(1 + \sum_{k=1}^{n}\sigma_{4_k}\phi_{mk}\right)^2}\right] \tag{15}$$

$$\beta_j = \frac{\bar{D}_{\text{eff},\,j/\text{mix}}}{(\bar{D}_{\text{eff}})_r} \tag{16}$$

$$\tau = 0 \qquad \phi_{mj} = 0 \qquad (1 > \eta \geq 0) \tag{17}$$

$$\eta = 1 \qquad \phi_{mj} = \phi_{bj} \qquad (\tau \geq 0) \tag{18}$$

$$\eta = 0 \qquad \frac{\partial \phi_{mj}}{\partial \eta} = 0 \qquad (\text{all } \tau) \tag{19}$$

Continuous bulk phase:

$$\frac{d\phi_{bj}}{d\tau} = -3\beta_j\sigma_{1_j}\left.\frac{\partial \phi_{mj}}{\partial \eta}\right|_{\eta = 1} \tag{20}$$

$$\tau = 0 \qquad \phi_{bj} = 1 \tag{21}$$

where, Eq. 16, $\bar{D}_{\text{eff},\,j/\text{mix}}$ is the mean effective diffusion coefficient for component j in a mixture of reactive solutes, $(\bar{D}_{\text{eff}})_r$ is a convenient mean effective diffusion coefficient used to nondimensionalize time, and the subscripted (j or k) dimensionless parameters are defined in a manner similar to those of the single-component system. To avoid confusion, it should be emphasized that ϕ_{mj} and ϕ_{bj} are normalized through division by the initial component concentration rather than by the initial total concentration of the mixture.

The single- and multiple-component equations are solved numerically (Bunge and Noble, 1984; Baird, 1985). Satisfaction of

the solute mass balance assures accuracy of the numerical solution.

Model comparisons

Preliminary model predictions presented earlier (Bunge and Noble, 1984) indicate that reaction reversibility does affect the solute extraction rate. The advancing front parameters, E and ϵ, can be related to the reversible reaction groups:

$$E = \frac{3\sigma_2\sigma_3}{\sigma_4} \tag{22}$$

$$\epsilon = \frac{3}{E}(\sigma_1 + \sigma_2) \tag{23}$$

The parameters σ_3 and σ_4 provide a quantitative measure of the applicability of the advancing front model. When σ_3 and σ_4 are both large or when only short dimensionless times are considered, the advancing front model is adequate and preferred for its simplicity. However, when both σ_3 and σ_4 are small, or for long times, the advancing front model overpredicts solute extraction. When reaction reversibility is important, the original molar ratio of reagent to solute is an insufficient criterion for specifying performance.

Extraction capacity

The concentration of solute A in the bulk phase after extensive contact with emulsion is found by overall material balance for all extracting species. The result written for a solute j is:

$$\phi^*_{bj} = \frac{1}{1 + \sigma_{1_j} + \sigma_{2_j}\left[1 + \dfrac{\sigma_{3_j}}{\left(1 + \sum_{k=1}^{n} \sigma_{4_k}\phi^*_{bk}\right)}\right]} \tag{24}$$

The final equilibrium concentration, ϕ^*_{bj}, is determined by simultaneous solution of Eq. 24 written for each component.

Representing the original mole ratio of internal reagent to bulk solute, $E/3$ indicates whether sufficient reagent has been provided for a particular extraction. For a solution of n solutes, a similar comparison of reagent to total extractable and reacting solute is given by

$$\frac{E_{\text{mix}}}{3} = \frac{1}{\sum_{j=1}^{n} 3/E_j} = \frac{1}{\sum_{j=1}^{n}\left(\dfrac{\sigma_{4j}}{\sigma_{2_j}\sigma_{3_j}}\right)} \tag{25}$$

As for single-solute extractions, Eq. 25 does not include the capacity of the membrane phase to extract solute.

Experimental Apparatus and Procedure

Experiments with initial bulk phase concentrations of 0.0025 and 0.0011 M were run for each of the four amines: aniline, 4-chloroaniline, and the *meta* and *para* isomers of toluidine. Mixtures of aniline and *p*-toluidine were studied at total amine concentrations of 0.0010 and 0.0020 M.

Batch extractions of amines were conducted in a 2L unbaffled glass extraction vessel with a variable speed 25 mm (2 in.) dia. turbine impeller. Amine concentrations were determined using a UV/visible spectrophotometer capable of performing multicomponent analysis. Emulsion globule diameters were determined photographically and expressed in terms of the area-averaged (Sauter mean) diameter (Baird, 1985).

Emulsion preparation

The membrane (oil) phase was 3 wt. % surfactant (nonionic polyamine, approx. mol wt. 1,000) and 97 wt. % isoparaffinic solvent (middle distillate, avg. mol wt. 384–404; viscosity 0.0425 Ns/m^2 at 22°C measured by a Cannon-Fenske Routine viscometer). The internal aqueous phase was 0.1 N in HCl.

Water-in-oil emulsions were prepared by first mixing together the oil and the surfactant. This membrane phase was then added to a blender along with the aqueous HCl and blended on the low setting for 2 min. The weight fraction of HCl solution in the emulsion was 0.40. The emulsion density was 870 kg/m^3.

Procedure

The prepared emulsion (66 mL) was added to 1L of deionized water stirred at 500 rpm. After emulsion addition, the globule diameter diminishes until a steady state value is reached; this required at least 5 minutes. Eight min after addition of the emulsion, a small volume (2–5 mL) of concentrated amine solution was injected (60,000–70,000 ppm). Since these concentrations exceed aqueous solubility limits, the amines are first dissolved in ethanol and then diluted with water to approximately 30 vol. % alcohol. This alcohol added to the bulk phase (about 1 mL) did not affect the partition coefficient values or extraction rates (Baird, 1985).

Samples of the bulk phase were periodically taken and the solute concentration determined from absorptions at wavelengths of 258, 260, 262, and 268 nm for aniline, *m*- and *p*-toluidine, and 4-chloroaniline, respectively. To separate the bulk phase from the emulsion, these samples flowed through filter paper sealed to the inside of the extraction vessel and covering a sampling spout. Sample volumes were kept as small as possible (2–3 mL) (Baird, 1985). Preliminary experiments measuring the pH of the external phase when no amine was present indicated that breakage was minimal.

Estimation of physical properties

Four physical properties of the solute emulsion system must be known to compare experimental and theoretical results: K, $\bar{D}_{\text{eff}}$, K_{mb}, and K_{mi}. Literature values of the dissociation constants for the four amines (at 25°C) are given in Table 1. Estimation of the mean effective diffusion coefficients, discussed previously (Bunge, 1984; Baird, 1985) and outlined in Appendix A, requires diffusion coefficients for the amine in both the mem-

Table 1. Reaction* and Phase Equilibria Values

Amine	K	K^0_{bm} Nonemulsion	K_{bm} ELM System
Aniline	42,740	0.60	1.7
m-Toluidine	53,700	1.00	3.9
p-Toluidine	120,200	1.00	3.9
4-Chloroaniline	14,000	—	5.8

*Weast (1973)

brane and internal phases, which are estimated using the Wilke-Chang correlation (Reid et al., 1977).

Measurement of partition coefficients

Phase partition coefficients were measured using two methods:

1. A nonemulsion system in which the two phases are mixed
2. A double emulsion system identical to that used for the extraction experiments, except that the aqueous internal HCl phase is replaced by deionized water.

For the ELM system, both external and internal phase equilibrium constants are required to define the system mass balance. Because of the difficulty in measuring the internal phase concentration, the internal and external phase partition coefficients are assumed to be equal. As long as solute activities in the two aqueous solutions are similar, K_{mb} and K_{mi} should be equal. The system mass balance,

$$C^{\circ}_{Ab}V_b = C^{*}_{Ab}V_b + C^{*}_{Am}V_m + C^{*}_{Ai}V_i \tag{26}$$

can be rearranged to give an expression for the bulk phase partition coefficient:

$$K_{mb} = [C^{\circ}_{Ab}V_b - C^{*}_{Ab}(V_b + V_i)]/C^{*}_{Ab}V_m \tag{27}$$

where C^{*}_{Ab}, C^{*}_{Am}, and C^{*}_{Ai} represent equilibrium concentrations in the respective phases. The external phase partition coefficient measured using the nonemulsion system will be denoted K°_{mb} to distinguish it from this K_{mb} value.

Results of measurements for the four amines studied are presented in Table 1. In each case, the values of f_m and f_b are approximately 0.64 and 0.94, respectively. The partition coefficient values measured using the ELM system appear to be significantly larger than those measured using the nonemulsion system.

The exact cause of this apparent increase in K_{mb} is not known and is presently under study. Teramoto et al. (1983) observed that membrane solubility of phenol and cresols increased with increased concentrations of their surfactant (sorbitan monoleate). However, this mechanism will not explain our results because nonemulsion experiments performed with and without surfactant produced the same value for K°_{mb}.

Two other possibilities, osmotic swelling and curvature effects can also be dismissed. Even if osmotic swelling occurs, the total volume of water ($V_b + V_i$) remains unchanged and according to Eq. 36 cannot contribute to variations in K_{mb}. Simple estimates of the Kelvin effect indicate that curvature will not significantly contribute to the phase equilibrium unless droplets diameters are 10 nm or smaller. Amine adsorption at the oil/water interfaces could explain difference between K_{mb} and K°_{mb}. These observations suggest that the usual nonemulsion distribution coefficient should be used with care. The predicted extraction values presented later use the K_{mb} measured by the ELM system with volume ratios similar to those in the extraction experiments.

Results and Discussion

Single-component studies

Results of extraction experiments for single components are presented in Figures 1–3. The dimensionless concentration, ϕ_b, is plotted as a function of dimensionless time, τ. For these experiments, R ranged between 0.3 and 0.4 mm and a τ of 2.0 corresponds to an actual time of 40–60 min (Baird, 1985). Experimental times are nondimensionalized using $\bar{D}_{eff}$, which includes reaction. Since the advancing front model assumes diffusion across the completely reacted shell, the nonreaction D_{eff} is appropriate and is used to calculate τ for the advancing-front predictions.

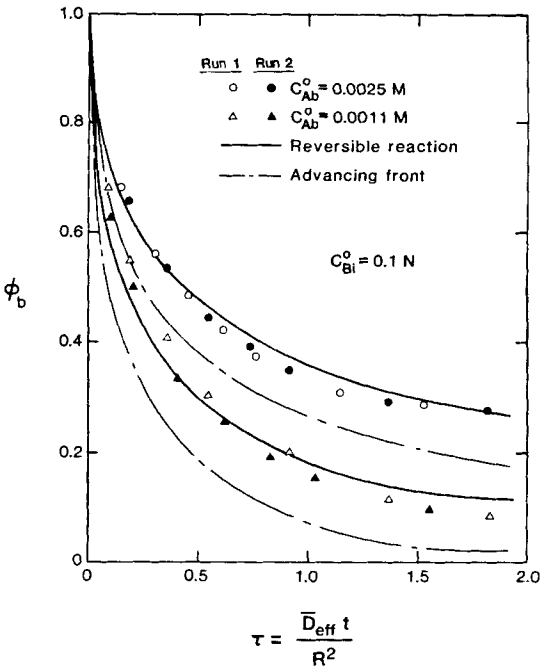

Figure 1. Experimental (symbols) and predicted extractions of aniline, K = 42,740, K_{mb} = 1.7.

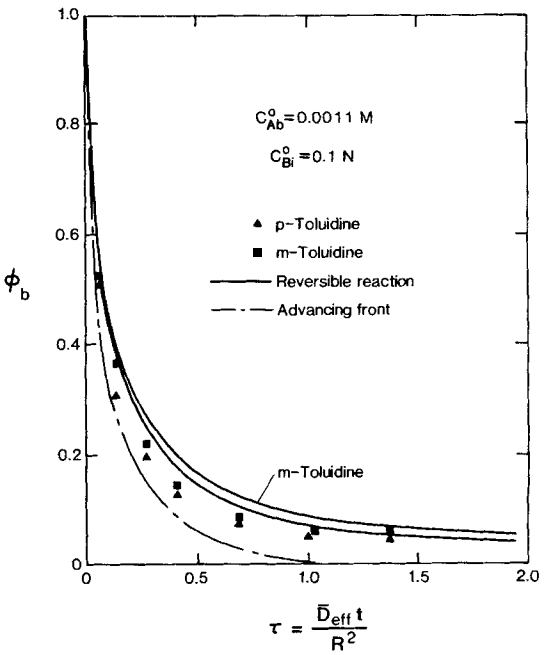

Figure 2a. Experimental (symbols) and predicted extractions of *m*-toluidine, K = 53,700, K_{mb} = 3.9, and of *p*-toluidine, K = 120,200, K_{mb} = 3.9.

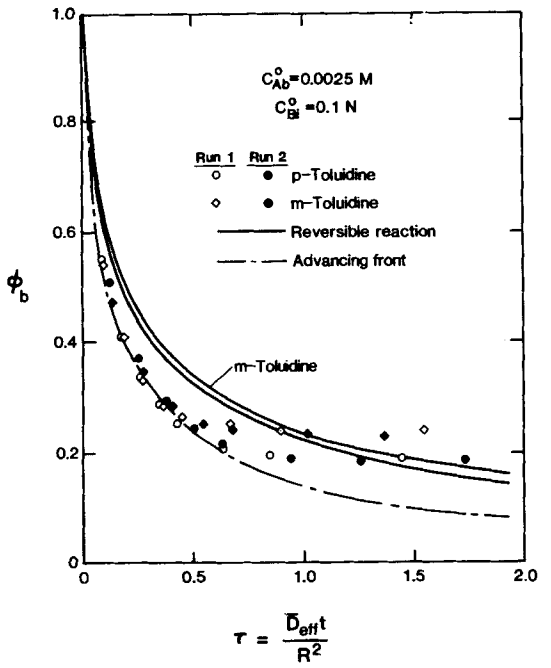

Figure 2b. Experimental (symbols) and predicted extractions of *m*-toluidine, $K = 53{,}700$, $K_{mb} = 3.9$, and of *p*-toluidine, $K = 120{,}200$, $K_{mb} = 3.9$.

The solid and open symbols in Figures 1–3 represent experimental data for two different runs and indicate that the reproducibility of the data with this experimental procedure is excellent. The solid and dashed curves represent the predictions of the reversible reaction and advancing front models, respectively.

The initial bulk phase amine concentrations are either 0.0025 or 0.0011 M. For the HCl concentration and volume ratios used in these experiments, there is sufficient acid to completely react all of the amine at the lower concentration ($E/3 = 2.21$) but insufficient to completely react all of the amine at the higher concentration ($E/3 = 0.97$). The dimensionless amine concentration for the 0.0011 M solution drops faster than for the 0.0025 M solution; to achieve an equivalent fractional extraction, the higher concentration solution must diffuse further into the globule.

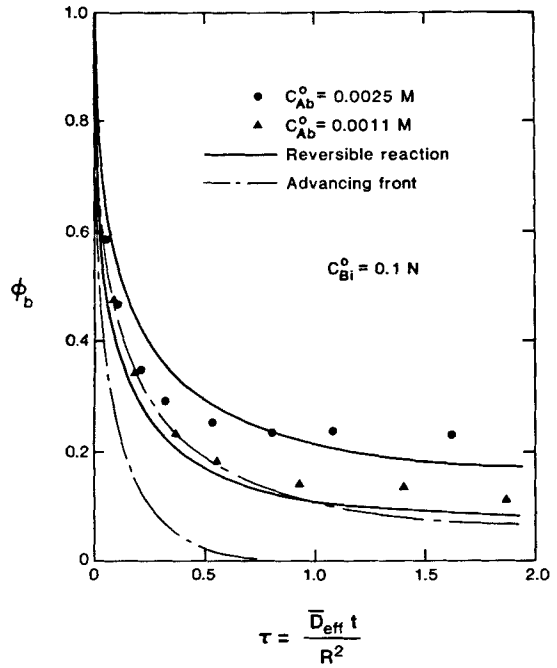

Figure 3. Experimental (symbols) and predicted extractions of 4-chloroaniline, $K = 1{,}410$, $K_{mb} = 5.8$.

The advancing front approach overpredicts the extraction rate of all four amines at both concentrations. In contrast with the experimental results, which always indicate a finite final equilibrium concentration, the advancing front model predicts a final concentration of zero for the 0.0011 M system because assuming reaction irreversibility requires the complete extraction of solute whenever the initial reagent mass exceeds that of the solute. This is best seen in Figures 2a and 3. In actuality, reaction reversibility always ensures a finite equilibrium value.

For the toluidines, Figures 2a and 2b, the advancing front model predictions are better than those for aniline, Figure 1, because the reaction with the toluidines is more nearly irreversible. In fact, the advancing front prediction for the 0.0025 M run is good up to a value of $\tau = 0.5$.

The reversible reaction approach underestimates toluidine extraction for dimensionless times less than one. The lumped-parameter distribution coefficient may be the source of this underprediction. If interfacial adsorption causes K_{mb} to differ from K^o_{mb}, then K_{mb} should vary as the extraction progresses and the solution concentration changes. Of the amines studied, toluidine extraction would be most sensitive to variations in K_{mb} because the sizable solubility and a large reaction constant cause phase equilibrium to control the initial extraction.

Comparing the experimental results shown in Figures 1–3, the toluidines and 4-chloroaniline extract faster than aniline, principally from greater amine solubility. Based on solubility alone, 4-chloroaniline should extract the fastest. However, a less favorable reaction slows the extraction rate to approximately that of the toluidines.

For the four amines studied, the advancing front predictions for 4-chloroaniline are the poorest, with the extraction rates overpredicted from the start. The differences between experimental results and the advancing front curves reflect the retarding effect of the low reaction equilibrium constant. The advancing front calculation assumes that all of the reagent is available to react, while reaction reversibility actually permits only a portion of the reagent to participate in solute extraction. In contrast, the reversible reaction model accounts for both reaction and phase equilibria to predict more closely the experimental extraction rates.

These results illustrate some important characteristics of the two models:

1. The advancing front model does an acceptable job of predicting extraction rates for solutes of high K for short times, but provides poor predictions for solutes with low K values or for long times.

2. The reversible reaction model is capable of accurately predicting extraction rates for systems with a wide range of K values.

Multicomponent extraction studies

In emulsion liquid membrane systems, the reacting species in a mixture of solutes compete for the available reagent. Binary

mixtures of aniline and *p*-toluidine were studied because sizable differences in both solubility and reaction reversibility are possible. Three mixtures of constant total amine concentration, respectively containing 25, 50, and 75% aniline, were prepared and the concentration of both amines was measured during the extraction process.

Results of the binary extraction experiments for initial total amine concentrations of 0.002 and 0.001 M are presented in Figures 4 and 5, respectively. The dimensionless concentration is defined as the concentration of species j divided by the initial concentration of species j, not the total initial concentration. Dimensionless time for the experimental data was determined using a concentration-averaged, reaction-adjusted effective diffusivity, $\bar{D}_{\text{eff,mix}}$ (see Appendix A), while the mixture-averaged, nonreaction diffusivity, $D_{\text{eff,mix}}$, was used for the advancing front model predictions.

Identical symbols are used to plot experimental aniline and *p*-toluidine concentrations of the same mixture; open symbols designate the concentration of toluidine, while solid symbols specify aniline. Reversible reaction predictions for the 25 and 75% aniline mixtures are shown as the broken and solid curves, respectively. Advancing front predictions, plotted as dashed curves, are calculated for each amine as for a single-component solution at the total initial amine concentration. The advancing front approach predicts separate curves for each component, reflecting their differing phase equilibria. Using the pure-component prediction for the total amine concentration assumes that the effect of *p*-toluidine on the extraction rate of aniline is the same as if *p*-toluidine behaves like aniline.

Analysis of the results presented in these two figures reveals that aniline extraction is retarded by the presence of *p*-toluidine.

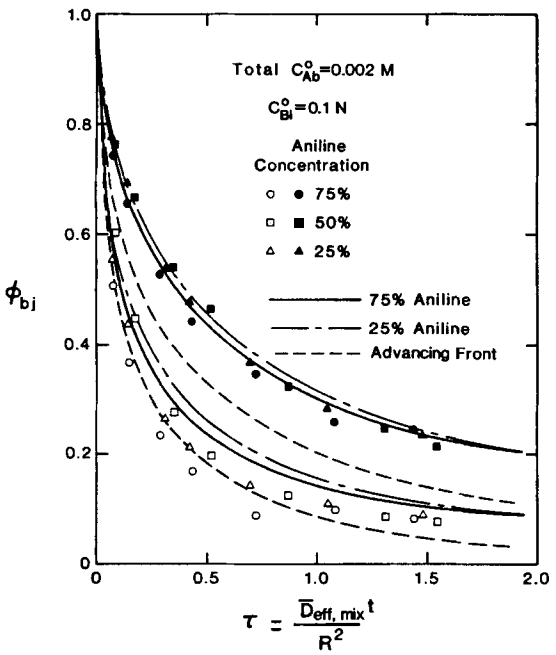

Figure 4. Experimental (symbols) and predicted extractions for mixtures of aniline and *p*-toluidine.
— and – – – Reversible-reaction predictions
----- Advancing-front predictions
● ■ ▲ Indicated aniline concentration
○ □ △ Balance concentration to 100% of *p*-toluidine

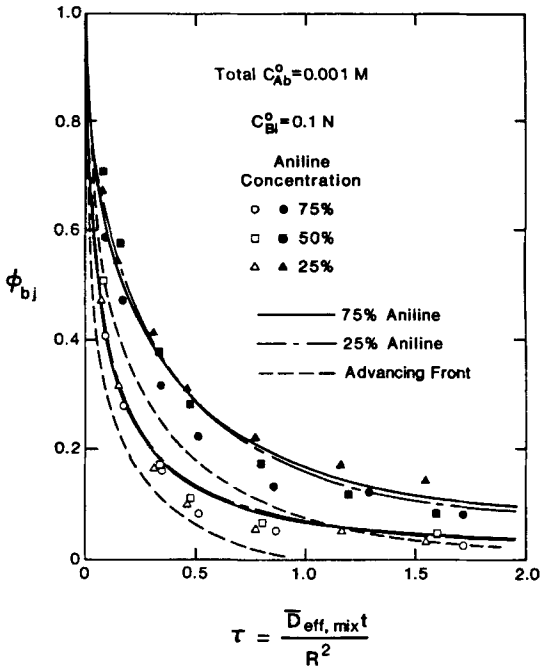

Figure 5. Experimental (symbols) and predicted extractions for mixtures of aniline and *p*-toluidine.
— and – – – Reversible-reaction predictions
----- Advancing-front predictions
● ■ ▲ Indicated aniline concentration
○ □ △ Balance concentration to 100% of *p*-toluidine

The single-component extraction studies show that the dimensionless solute concentration drops more quickly for solutions of lower initial concentrations. However, in these studies, the dimensionless concentrations of aniline and *p*-toluidine extract at nearly the same rate for all mixtures at the same total concentration. This means that the more soluble *p*-toluidine is able to penetrate the emulsion globule more quickly than the aniline and partially consume the available reagent. The aniline must therefore compete with the *p*-toluidine for the available reagent, which significantly slows its extraction rate. The advancing front prediction reasonably represents *p*-toluidine extraction, but considerably overestimates the extent of aniline removal. While somewhat conservative for *p*-toluidine, the reversible reaction theory acceptably predicts the experimental extraction performance at both concentrations.

Multicomponent extraction of dissimilar species

The component extraction rates of mixtures should be strongly influenced by mixture composition when the species have dissimilar phase and reaction equilibria. Figures 6 through 9 illustrate this effect for several hypothetical mixtures calculated using the multicomponent model. The mean effective diffusivities of the two hypothetical components are assumed to be identical (i.e., $\beta_1 = \beta_2 = 1$).

Figure 6 compares the extraction rates of two components with identical phase equilibria ($\sigma_1 = 0.0221$ and $\sigma_2 = 0.0242$ for both) and varying reaction equilibria. The initial ratio of reagent to solute concentrations for both components is fixed at $\sigma_{3j}/\sigma_{4j} = 50$. The concentration and reaction equilibrium of

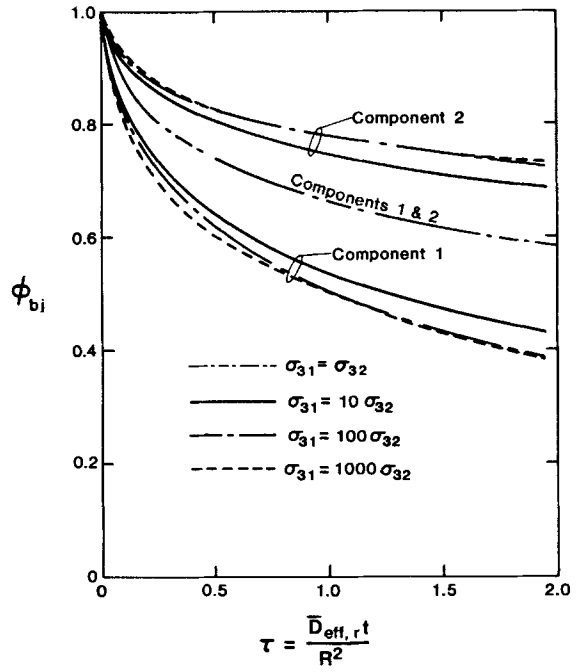

Figure 6. Reversible-reaction multicomponent model predictions of binary component extraction for constant identical phase equilibria and varying reaction equilibria.

$\sigma_{11} = \sigma_{12} = 0.0221$
$\sigma_{21} = \sigma_{22} = 0.0242$
$\sigma_{32} = 500$
$\sigma_{42} = 10$
$\sigma_{31}/\sigma_{41} = 50$

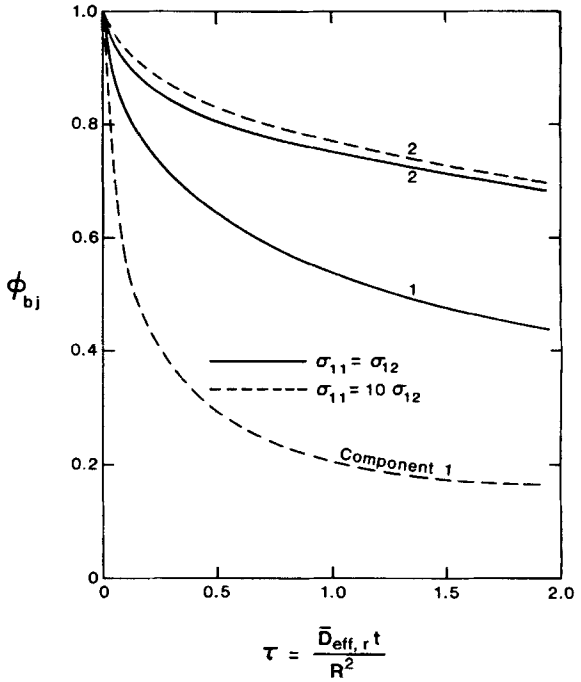

Figure 7. Reversible-reaction multicomponent model predictions of binary component extraction for constant reaction equilibria and varying phase equilibria.

$\sigma_{12} = 0.0221$
$\sigma_{21} = \sigma_{22} = 0.0242$
$\sigma_{31} = 5{,}000$
$\sigma_{41} = 100$
$\sigma_{32} = 500$
$\sigma_{42} = 10$

component 2, the more reversible species, are held constant ($\sigma_{32} = 500$ and $\sigma_{42} = 10$) while K_1 is varied from 1 to 1,000 times K_2. When the K value of the more irreversible species (K_1) is increased the extraction rate of the more reversible component is depressed. We also note that for extremely large values of K_1 the extraction is phase-equilibrium controlled and further increases in K_1 produce little effect. This same effect of large K is also seen for single-component solutions (Bunge and Noble, 1984).

Figures 7 and 8 compare the extraction rates of two components with unchanging reaction equilibria ($\sigma_{31} = 5{,}000$, $\sigma_{41} = 100$, $\sigma_{32} = 500$, $\sigma_{42} = 10$) and varying phase equilibria. The phase equilibrum for component 2 is held constant at $\sigma_{12} = 0.0221$. In Figure 7, the component favored by reaction equilibria, component 1, is equal to or favored over component 2 by phase equilibria ($\sigma_{11} \geqq \sigma_{12}$). For the parameters used here, improving the phase equilibria for component 1 significantly accelerated its extraction while only slightly depressing the extraction of component 2.

Figure 8 demonstrates what happens when the component favored by reaction equilibria is unfavored by phase equilibria ($\sigma_{11} < \sigma_{12}$). When reaction reversibility and phase equilibrium create opposing effects, as in Figure 8, the component favored by reaction (component 1) can extract more slowly than the unfavored component (component 2).

Figure 9 shows a more extreme case of the situation in Figure 8. The more irreversible component species 1 ($K_1 = 1{,}000\ K_2$) has the smaller phase equilibria. In this situation the more soluble component (species 2) initially extracts much faster than component 1. However, as extraction of the less soluble component 1 proceeds, it begins to force the reaction product of component 2 to generate A_2,

$$P_2 + A_1 \overset{K_1/K_2}{\rightleftharpoons} P_1 + A_2 \tag{28}$$

which then diffuses back into the bulk phase. This creates the minimum in the extraction history curve seen for component 2 in Figure 9. This phenomenon was observed experimentally by Terry et al. (1981) for a phenol-acetic acid mixture. In their system, phenol was significantly more soluble than acetic acid, while acetic acid dissociation ($K = 1.8 \times 10^9$) was considerably stronger than that for phenol (1.1×10^4). Notably, advancing front models would not predict such an occurrence.

The experimental and predicted results shown in Figures 4–9 demonstrate that reaction and phase equilibria can profoundly influence extraction of mixed solutes. For some combinations of reaction and phase equilibria, treating a mixture as a single, lumped component will not be adequate because extraction of a given species is influenced by the presence of others. In some cases differences in extraction rates could be used to separate components. Interference by mixture components can also be a problem if the solute targeted for removal has a smaller reaction equilibrium constant than other extractable species that are present.

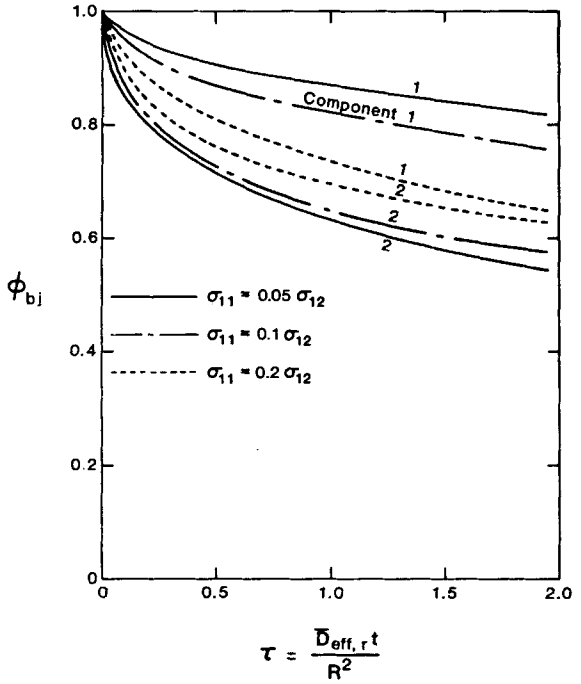

Figure 8. Reversible-reaction multicomponent model predictions of binary component extraction for constant reaction equilibria and varying phase equilibria.

$\sigma_{12} = 0.0221$
$\sigma_{21} = \sigma_{22} = 0.0242$
$\sigma_{31} = 5{,}000$
$\sigma_{41} = 100$
$\sigma_{32} = 500$
$\sigma_{42} = 10$

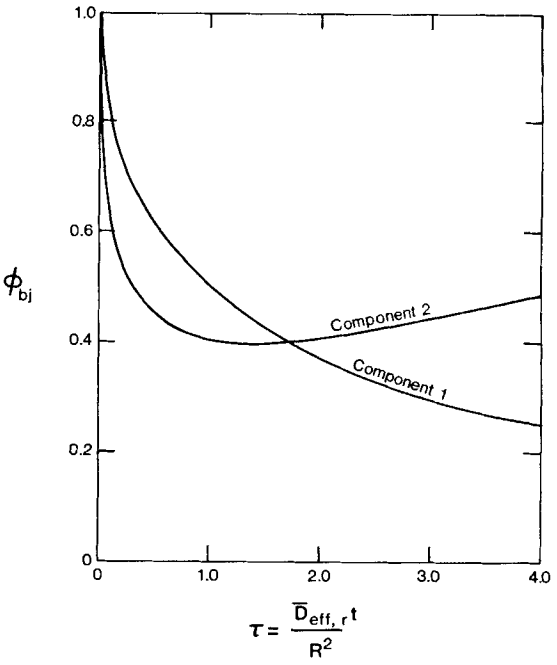

Figure 9. Reversible-reaction multicomponent model prediction of binary component extraction when the more soluble component 2 has the more reversible reaction.

$\sigma_{11} = 0.0221$
$\sigma_{21} = 0.221$
$\sigma_{21} = \sigma_{22} = 0.0242$
$\sigma_{31} = 5(10^5)$
$\sigma_{32} = 500$
$\sigma_{41} = 10^4$
$\sigma_{42} = 10$

Conclusions

This paper reports a substantial body of experimental data that can be used to test theoretical models. Extraction results for several amines demonstrate that reversibility of the acid-amine reaction along with amine solubility in the membrane phase affect extraction rates. The reversible reaction model presented earlier by Bunge and Noble satisfactorily predicts these experimental results, using only independently measured parameters.

The reversible reaction model has been extended to mixture extractions with good success. This model is used to investigate the contributions of various system parameters. For multicomponent extractions, competition between reacting species retards the individual extraction rates. If the species reaction and phase equilibria are greatly dissimilar, the effects can be pronounced, and concentration minimums may be observed.

Interfacial adsorption may significantly contribute to the overall amine extraction. Traditional, nonemulsion methods of measuring partition coefficients are unable to account for this increased globule solute capacity for solute. Therefore, we used ELM systems to measure the apparent distribution between phases. The resulting partition coefficients are lumped parameters incorporating all effects leading to the apparent sorption of solute.

Acknowledgment

This work was supported in part by the Environmental Protection Agency under Grant No. R811247-01-0. R. S. Baird acknowledges support from the National Bureau of Standards through a cooperative agreement (NB83RAH 30001). The assistance of Daniel L. Reed with some of the computer calculations was greatly appreciated.

Notation

A = solute
B = reagent
C_{Ab} = bulk phase solute concentration, M
C_{Ai} = internal phase solute concentration, M
C_{Am} = membrane phase solute concentration, M
C_{Bi} = internal phase reagent concentration, N
C_{Pi} = internal phase product concentration, M
D_{eff} = effective solute diffusivity in emulsion globule based on membrane driving force and including concentration-dependent reaction effects (Appendix A), m^2/s
$\bar{D}_{eff}$ = mean effective solute diffusivity in emulsion globule based on membrane phase driving force and including reaction effects (Appendix A), m^2/s
D = solute diffusion coefficient, m^2/s
$E/3$ = original molar ratio of reagent to solute
f_b = bulk volume fraction of total volume
f_m = membrane volume fraction of emulsion
K = reaction equilibrium constant, M^{-1}
K_{mb} = partition coefficient between membrane and bulk phases, C_{Am}/C_{Ab}
K_{mi} = partition coefficient between membrane and internal phases, C_{Am}/C_{Ab}
n = total number of components in mixture
r = radial coordinate, cm
P = product of reaction between A and B
R = average globule radius, cm; experimentally, R is equal to one-half the Sauter mean diameter
t = time, s
V = phase volume, mL

Greek letters

β = diffusion coefficient ratio
γ = diffusion enhancement factor
ϵ = perturbation parameter in advancing-front model
η = normalized radial coordinate
σ_1 = dimensionless parameter
σ_2 = dimensionless parameter
σ_3 = dimensionless reagent concentration
σ_4 = dimensionless solute concentration
τ = dimensionless time
ϕ = normalized solute concentration
ψ = parameter, Eq. 15

Subscripts

A = solute
b = continuous bulk phase
B = reagent
i = internal phase
j = chemical species of interest in mixture
k = chemical species in mixture
mix = mixture of extracting solutes
m = membrane phase
P = reaction product
r = reference
tot = total

Superscripts

° = initial concentration; in the case of partition coefficients, refers to nonemulsion system.
* = equilibrium concentration

Appendix A. Calculation of Mean Effective Diffusivity

Based on the membrane driving force, the mean effective diffusivity, $\bar{D}_{\text{eff}}$, includes contributions from diffusion of solute through the membrane phase as well as diffusion of both reacted and unreacted solutes through the internal phase. Diffusion through the internal phase can be consequential when the internal phase molecular diffusion coefficient is significantly larger than the membrane phase coefficient, or when solute reaction induces large solute concentrations in the internal phase relative to those in the membrane phase.

The calculation of the mean effective diffusion coefficient for diffusion through a reacting composite medium was discussed previously (Bunge and Noble, 1984; Baird, 1985). Following Ho et al. (1981) we calculate the effective globule diffusivity using the Jefferson-Witzell-Sibbet equation through a composite medium (Crank, 1977; Jefferson et al., 1958), where the apparent internal phase diffusivity of both reacted and unreacted solute is estimated from an enhancement of the molecular diffusity of unreacted solute (γD_i):

$$\gamma = 1 + \frac{\sigma^3}{(1 + \sigma_4\phi_m)^2} \tag{A1}$$

If no reaction occurs, σ_3 is zero and γ equals one. Membrane and internal phase diffusivities are estimated using the Wilke-Chang correlation with molecular volumes calculated from the Le Bas additive method (Reid, 1977).

The effective diffusion coefficient depends on the local membrane concentration, ϕ_m, and the original concentrations of solute and reagent indicated by ϕ_3 and σ_4. Because the sensitivity of D_{eff} to changes in ϕ_m is not large, and because tremendous mathematical complexity arises by allowing D_{eff} to vary with ϕ_m, we use $\bar{D}_{\text{eff}}$ at its mean value over the range of ϕ_m varying from 0 to 1. At a fixed mole ratio of reagent to solute, $\bar{D}_{\text{eff}}$ approaches the no-reaction $\bar{D}_{\text{eff}}$ for large or small values of σ_3 (Bunge and Noble, 1984).

Table A1. Values of Parameters Used to Calculate β_j in Figures 4 and 5*

Parameter	Aniline	*p*-Toluidine	Mixture
C°_{Ab}, M	0.0015	0.0005	0.0020
$D_i \times 10^{10}$, m^2/s	9.32	8.35	9.08
$D_m \times 10^{11}$, m^2/s	5.83	5.22	5.68
K_{mi}	1.7	3.9	2.25
σ_3	4,274	12,020	6,210
σ_4	85.5	240.4	124.2
$\bar{D}_{\text{eff}}(j/\text{mix or mix}) \times 10^{10}$, m^2/s	1.5	1.11	1.43
β_j	1.10	0.777	1.00

*$\bar{D}_{\text{eff},r} = \bar{D}_{\text{eff,mix}}$

Effective diffusivity for multicomponent mixtures

The effective diffusivity of multicomponent mixtures is affected by competition between the species for the available reagent. To handle this in a manner analogous to the single-component method results in an extremely complicated expression for the multicomponent enhancement factor. For this reason, a simpler approach was adopted. We use concentration-averaged parameters for the variables needed to calculate an overall mixture $D_{\text{eff,mix}}$ ($\sigma_{3,\text{mix}}$, $\sigma_{4,\text{mix}}$, $D_{i,\text{mix}}$, $D_{m,\text{mix}}$, $K_{mi,\text{mix}}$) used as reference (Baird, 1985):

$$(\text{Parameter})_{\text{mix}} = \frac{\sum_{j=1}^{n} (\text{Parameter})(C^\circ_{Ab})_j}{\sum_{j=1}^{n} (C^\circ_{Ab})_j} \tag{A2}$$

where the values of σ_{4j} are calculated using $C^\circ_{Ab,\text{tot}}$ and not the actual original concentration of component j. The mean value, $\bar{D}_{\text{eff,mix}}$, is then determined over the range of ϕ_m varying from zero to one as was done for the single solute.

The model calculations for mixtures require specification of a mean effective diffusion coefficient for component j in this mixture of solutes, $\bar{D}_{\text{eff},j/\text{mix}}$. The concentration-dependent coefficient is found by following the procedure for single solutes using σ_{3j}, σ_{4j}, D_{ij}, D_{mj}, and K_{imj}, where σ_{4j} is based on the total concentration of reactive solutes, $C^\circ_{Ab,\text{tot}}$. The mean value is computed for ϕ_{mj} varying between zero and one. Table A1 illustrates these calculations for an example case of 75% aniline in the 0.002 M solution.

Literature cited

Baird, R. S., "An Experimental Study of Amine Extraction Using Emulsion Liquid Membranes," M.S. Thesis, Colorado School of Mines (1985).

Bunge, A. L., and R. D. Noble, "A Diffusion Model for Reversible Consumption in Emulsion Liquid Membranes," *J. Membrane Sci.*, **21**, 55 (1984).

Crank, J., *The Mathematics of Diffusion*, 2nd ed., Clarendon Press, Oxford, Ch. 12 (1977).

Fales, J. L., and P. Stroeve, "A Perturbation Solution for Batch Extrac-

tion with Double Emulsions: Role of Continuous-Phase Mass Transfer Resistance," *J. Membrane Sci.*, **21,** 35 (1984).
Ho, W. S., T. A. Hatton, E. N. Lightfoot, and N. N. Li, "Batch Extraction with Liquid Surfactant Membranes: A Diffusion-Controlled Model," *AICHE J.*, **28,** 662 (1982).
Jefferson, T. B., O. W. Witzell, and W. L. Sibbit, "Thermal Conductivity of Graphite-Silicone Oil and Graphite-Water Suspensions," *Ind. Eng. Chem.*, **50,** 1589 (1958).
Kim, K. S., S. J. Choi, and S. K. Ihm, "Simulation of Phenol Removal from Wastewater by Liquid Membrane Emulsion," *Ind. Eng. Chem.*, **22,** 167 (1983).
Li, N. N., "Separating Hydrocarbons with Liquid Membranes," U.S. Patent 3,410,794 (1968).
Reid, R. C., J. M. Prausnitz, and T. K. Sherwood, *The Properties of Gases and Liquids*, 3rd ed., McGraw-Hill, New York (1977).
Skelland, A. H. P., and J. M. Lee, "Drop Size and Continuous-Phase Mass Transfer in Agitated Vessels," *AICHE J.*, **27,** 99 (1981).
Stroeve, P., and P. P. Varanasi, "Extraction with Double Emulsions in a Batch Reactor: Effect of Continuous-Phase Resistance," *AIChE J.*, **30,** 1007 (1984).
Teramoto, M., H. Takihana, M. Shibutani, T. Yuasa, Y. Miyake, and H. Teranishi, "Extraction of Amine by W/O/W Emulsion System," *J. Chem. Eng. Japan.*, **14,** 122 (1981).
Teramoto, M., H. Takihana, M. Shibutani, T. Yuasa, and N. Hara, "Extraction of Phenol and Cresol by Liquid Surfactant Membrane," *Sep. Sci. Technol.*, **18,** 397 (1983).
Terry, R. E., N. N. Li, and W. S. Ho, "Extraction of Phenolic Compounds and Organic Acids by Liquid Membranes," *J. Membrane Sci.*, **10,** 305 (1982).
Weast, R. C., ed., *Handbook of Chemistry and Physics*, 54th ed., CRC Press, Cleveland, OH (1973).

Manuscript received Sept. 12, 1985, and revision received April 7, 1986.